



# The Dependence of Iron-rich Metal-poor Star Occurrence on Galactic Environment Supports an Origin in Thermonuclear Supernova Nucleosynthesis

Zachary Reeves<sup>1</sup> , Kevin C. Schlafman<sup>1</sup> , and Henrique Reggiani<sup>2,3</sup> <sup>1</sup> William H. Miller III Department of Physics and Astronomy, Johns Hopkins University, 3400 N. Charles St, Baltimore, MD 21218, USA; [zackreeves96@gmail.com](mailto:zackreeves96@gmail.com)<sup>2</sup> The Observatories of the Carnegie Institution for Science, 813 Santa Barbara St, Pasadena, CA 91101, USA

Received 2023 January 31; revised 2023 June 27; accepted 2023 July 10; published 2023 August 25

## Abstract

It has been suggested that a class of chemically peculiar metal-poor stars called iron-rich metal-poor (IRMP) stars formed from molecular cores with metal contents dominated by thermonuclear supernova nucleosynthesis. If this interpretation is accurate, then IRMP stars should be more common in environments where thermonuclear supernovae were important contributors to chemical evolution. Conversely, IRMP stars should be less common in environments where thermonuclear supernovae were not important contributors to chemical evolution. At constant  $[\text{Fe}/\text{H}] \lesssim -1$ , the Milky Way's satellite classical dwarf spheroidal (dSph) galaxies and the Magellanic Clouds have lower  $[\alpha/\text{Fe}]$  than the Milky Way field and globular cluster populations. This difference is thought to demonstrate the importance of thermonuclear supernova nucleosynthesis for the chemical evolution of the Milky Way's satellite classical dSph galaxies and the Magellanic Clouds. We use data from the Sloan Digital Sky Survey Apache Point Observatory Galactic Evolution Experiment and Gaia to infer the occurrence of IRMP stars in the Milky Way's satellite classical dSph galaxies  $\eta_{\text{dSph}}$  and the Magellanic Clouds  $\eta_{\text{Mag}}$ , as well as in the Milky Way field  $\eta_{\text{MWF}}$  and globular cluster populations  $\eta_{\text{MWGC}}$ . In order of decreasing occurrence, we find  $\eta_{\text{dSph}} = 0.07^{+0.02}_{-0.02}$ ,  $\eta_{\text{Mag}} = 0.037^{+0.007}_{-0.006}$ ,  $\eta_{\text{MWF}} = 0.0013^{+0.0006}_{-0.0005}$ , and a  $1\sigma$  upper limit  $\eta_{\text{MWGC}} < 0.00057$ . These occurrences support the inference that IRMP stars formed in environments dominated by thermonuclear supernova nucleosynthesis and that the time lag between the formation of the first and second stellar generations in globular clusters was longer than the thermonuclear supernova delay time.

*Unified Astronomy Thesaurus concepts:* [Chemical enrichment \(225\)](#); [Chemically peculiar stars \(226\)](#); [Dwarf spheroidal galaxies \(420\)](#); [Galactic archaeology \(2178\)](#); [Globular star clusters \(656\)](#); [Large Magellanic Cloud \(903\)](#); [Magellanic Clouds \(990\)](#); [Milky Way Galaxy \(1054\)](#); [Population II stars \(1284\)](#); [Small Magellanic Cloud \(1468\)](#); [Stellar abundances \(1577\)](#); [Type Ia supernovae \(1728\)](#)

*Supporting material:* machine-readable table

## 1. Introduction

Thermonuclear supernovae<sup>4</sup> are prolific producers of iron-peak elements with a theoretically predicted average stable yield of more than  $0.6 M_{\odot}$  of iron-peak elements but much less of the  $\alpha$  and light odd- $Z$  elements. This is in sharp contrast to core-collapse supernovae that produce  $\alpha$  and light odd- $Z$  elements in roughly the solar ratios but with relatively little iron-peak production (e.g., Sukhbold et al. 2016).

Based on a compilation of theoretical stable nucleosynthetic yields predicted by a variety of thermonuclear supernova progenitor channels (i.e., single degenerate and double degenerate) and explosion mechanisms (e.g., pure detonations, pure deflagrations, delayed detonations, double detonations, etc.), Reggiani et al. (2023) proposed the existence of a new class of chemically peculiar metal-poor stars with  $[\text{Fe}/\text{H}] \lesssim -1$  and  $[\text{O}, \text{F}, \text{Ne}, \text{Na}, \text{Mg}, \text{Al}, \text{Cl}, \text{K}, \text{Co}, \text{Cu}, \text{Zn}/\text{Fe}] < 0$  formed from molecular cores with metal contents dominated by

thermonuclear supernova nucleosynthesis.<sup>5</sup> They called stars with these properties iron-rich metal-poor (IRMP) stars, as this part of elemental abundance space is consistent with thermonuclear supernova nucleosynthesis but rarely observed in metal-poor stars. They argued that if their interpretation is correct, then IRMP stars should be more common in environments where thermonuclear supernovae were relatively more important contributors to chemical evolution relative to core-collapse supernovae (e.g., environments with long star formation durations). On the other hand, they argued that in environments where thermonuclear supernovae were not important contributors to chemical evolution relative to core-collapse supernovae (e.g., environments with short star formation durations) IRMP stars should be less common.

One way to test this prediction would be to compare the relative occurrence of IRMP stars in the Milky Way's field population, its globular clusters, its satellite classical dwarf spheroidal (dSph) galaxies, and the Magellanic Clouds. At constant spectroscopically inferred metallicities  $[\text{Fe}/\text{H}] \lesssim -1$ ,<sup>6</sup> both the Milky Way's classical dSph satellites (Shetrone et al. 2001, 2003;

<sup>3</sup> Carnegie Fellow.

<sup>4</sup> In this article we use the phrase “thermonuclear supernovae” to refer to the theoretical concept of electron-degenerate carbon–oxygen white dwarfs experiencing runaway carbon fusion that releases enough energy to gravitationally unbind the white dwarfs and thereby cause explosions.

<sup>5</sup> The yields in that compilation came from Seitzzahl et al. (2013, 2016), Fink et al. (2014), Ohlmann et al. (2014), Papish & Perets (2016), Leung & Nomoto (2018, 2020a, 2020b), Nomoto & Leung (2018), Bravo et al. (2019), Boos et al. (2021), Gronow et al. (2021a, 2021b), and Neopane et al. (2022).

<sup>6</sup> In this article metallicity  $[\text{Fe}/\text{H}]$  has its usual meaning,  $[\text{Fe}/\text{H}] = \log_{10}(N_{\text{Fe}}/N_{\text{H}})_{*} - \log_{10}(N_{\text{Fe}}/N_{\text{H}})_{\odot}$ , where  $N_X$  are the logarithmic number densities of atoms of an element  $X$  in a stellar photosphere and  $N_{\text{H}} \equiv 12$ .

Tolstoy et al. 2003; Kirby et al. 2009, 2010, 2011a, 2011b) and the Magellanic Clouds (Pompéia et al. 2008; Van der Swaelmen et al. 2013; Nidever et al. 2020) have lower spectroscopically inferred ratios of the  $\alpha$ -elements oxygen, magnesium, silicon, and calcium to iron  $[\alpha/\text{Fe}]^7$  than the Milky Way (e.g., Wallerstein 1962; Luck & Bond 1981; Peterson 1981; Gratton 1983; Luck & Bond 1985; Magain 1985; Gratton & Ortolani 1986; Gratton & Sneden 1988; Magain 1989; Ryan et al. 1991; McWilliam et al. 1995a, 1995b) and its globular clusters (e.g., Cohen 1978, 1979, 1980, 1981; Pilachowski et al. 1983). These offsets in  $[\alpha/\text{Fe}]$  between the Milky Way field and globular cluster populations and between its satellite classical dSph galaxies and the Magellanic Clouds are usually understood to indicate the longer durations of low-metallicity star formation and therefore the relatively more important contributions of thermonuclear supernovae to the chemical evolution of the latter two environments at low metallicities (e.g., Lanfranchi & Matteucci 2003, 2004; Lanfranchi et al. 2006; Marcolini et al. 2006; Lanfranchi & Matteucci 2007; Lanfranchi et al. 2008; Kirby et al. 2011a; Bekki & Tsujimoto 2012; Nidever et al. 2020; Reggiani et al. 2021). If the Reggiani et al. (2023) interpretation of IRMP stars is valid, then IRMP stars should be less common in the Milky Way field and globular cluster populations than in its satellite classical dSph galaxies and the Magellanic Clouds.

The nitrogen, sodium, and aluminum abundances of individual stars in globular clusters have been found to be anticorrelated with the carbon, oxygen, and magnesium abundances in the same stars. These abundance anticorrelations have been interpreted as evidence for multiple generations of star formation in globular clusters (e.g., Sneden et al. 1992; Gratton et al. 2001, 2004; Carretta et al. 2009; Bastian & Lardo 2018). The Reggiani et al. (2023) interpretation of IRMP stars also suggests the possibility that the occurrence of IRMP stars in globular clusters can be used to constrain the time lag between the formation of a globular cluster’s first and second stellar generations. For Type Ia supernovae<sup>8</sup> delay times  $\tau_{\text{Ia}} \lesssim 100$  Myr, the Type Ia supernova rate  $\Phi_{\text{Ia}}$  has the value  $\Phi_{\text{Ia}} \sim 10^{-12} \text{ yr}^{-1} M_{\odot}^{-1}$  (e.g., Totani et al. 2008; Maoz et al. 2011, 2012; Graur et al. 2014; Maoz et al. 2014). Assuming that rate and a typical first-generation initial globular cluster mass  $M_{\text{MWGC}} \sim 10^6 M_{\odot}$  (e.g., Conroy 2012), order 10 Type Ia supernovae should occur in a newly formed globular cluster every 10 Myr after the Type Ia delay time has elapsed. While the occurrence of the short-period binaries necessary to produce most of the theoretically predicted thermonuclear supernova progenitor systems is a factor of about three lower in globular clusters’ first generations than in the field (Carney et al. 2003; Lucatello et al. 2015), after the Type Ia supernovae delay times have elapsed a few thermonuclear explosions should occur every 10 Myr during the formation of a globular cluster. The Reggiani et al. (2023) interpretation of IRMP stars therefore implies that if the time lag between the formation of first- and second-generation stars in globular clusters was shorter than the typical thermonuclear supernova delay time,

then the occurrence of IRMP stars in globular clusters should be significantly lower than in the Milky Way field. If the time lag between the formation of first- and second-generation stars in globular clusters is longer than the typical thermonuclear supernova delay time, then the occurrence of IRMP stars in globular clusters and the Milky Way field should be comparable.

We argue that if the Reggiani et al. (2023) interpretation of the origin of IRMP stars is accurate, then the occurrence of IRMP stars in the Milky Way field population  $\eta_{\text{MWf}}$ , the Magellanic Clouds  $\eta_{\text{Mag}}$ , and the Milky Way’s satellite classical dSph galaxies  $\eta_{\text{dSph}}$  should be ordered  $\eta_{\text{MWf}} < \eta_{\text{Mag}} \sim \eta_{\text{dSph}}$ . If the time lag between the formation of the first and second generations in globular clusters was shorter than the thermonuclear supernova delay time, then the occurrence of IRMP stars in the Milky Way globular cluster population  $\eta_{\text{MWGC}}$  should be  $\eta_{\text{MWGC}} \lesssim \eta_{\text{MWf}} < \eta_{\text{Mag}} \sim \eta_{\text{dSph}}$ . If the time lag between the formation of the first and second generations in globular clusters was longer than the thermonuclear supernova delay time, then  $\eta_{\text{MWGC}} \sim \eta_{\text{MWf}} < \eta_{\text{Mag}} \sim \eta_{\text{dSph}}$ . In this article, we calculate the occurrence of IRMP stars in the Milky Way’s satellite classical dSph galaxies, the Magellanic Clouds, the Milky Way field population, and the Milky Way’s globular clusters. We describe in Section 2 the assembly of our analysis samples and quantify in Section 3 the occurrence of IRMP stars in each environment. We review the implications of those occurrences in Section 4 and conclude by summarizing our findings in Section 5.

## 2. Data

To calculate the occurrence of IRMP stars in the Milky Way’s satellite classical dSph galaxies, the Magellanic Clouds, the Milky Way field population, and the Milky Way’s globular clusters, we use data derived from spectra that were gathered during the third and fourth phases of the Sloan Digital Sky Survey (SDSS; Eisenstein et al. 2011; Blanton et al. 2017) as part of its Apache Point Observatory Galactic Evolution Experiment (APOGEE; Majewski et al. 2017). These spectra were collected with the APOGEE spectrographs (Zasowski et al. 2013, 2017; Wilson et al. 2019; Beaton et al. 2021; Santana et al. 2021) on the New Mexico State University 1 m Telescope (Holtzman et al. 2010), the Sloan Foundation 2.5 m Telescope (Gunn et al. 2006), and the 2.5 m Irénée du Pont Telescope (Bowen & Vaughan 1973). As part of SDSS Data Release (DR) 17 (Abdurro’uf et al. 2022), these spectra were reduced and analyzed with the APOGEE Stellar Parameter and Chemical Abundance Pipeline (ASPCAP; Allende Prieto et al. 2006; Holtzman et al. 2015; Nidever et al. 2015; García Pérez et al. 2016) using an *H*-band line list, MARCS model atmospheres, and model-fitting tools optimized for the APOGEE effort (Alvarez & Plez 1998; Gustafsson et al. 2008; Hubeny & Lanz 2011; Plez 2012; Smith et al. 2013; Cunha et al. 2015; Shetrone et al. 2015; Jönsson et al. 2020; Smith et al. 2021).

We use the CasJobs portal<sup>9</sup> and the query described in the Appendix to generate our initial sample of photospheric stellar parameters and elemental abundances for giant stars with  $\log g < 3.8$ . As described in the Appendix, we use a carefully curated set of data quality flags to ensure the accuracy and precision of those photospheric stellar parameters and elemental abundances. We set to null any elemental abundance/

<sup>7</sup> In this article the  $\alpha$ -element-to-iron ratio  $[\alpha/\text{Fe}]$  has its usual meaning,  $[\alpha/\text{Fe}] = \log_{10}(N_{\alpha}/N_{\text{Fe}})_{*} - \log_{10}(N_{\alpha}/N_{\text{Fe}})_{\odot}$ , where  $\alpha$  is the sum of some subset of the elements oxygen, magnesium, silicon, and calcium.

<sup>8</sup> In this article we use the phrase “Type Ia supernovae” to refer to the electromagnetic transients empirically classified as Type Ia supernovae based on their observed properties.

<sup>9</sup> <http://skyserver.sdss.org/casjobs/>

elemental abundance uncertainty pair that does not pass the data quality checks described in the Appendix. Corrections for departures from local thermodynamic equilibrium are usually small for  $H$ -band elemental abundance inferences (e.g., Osorio et al. 2020), and we choose not to apply them in our analysis.

Following Reggiani et al. (2023), we define an IRMP star as a star with  $[\text{Fe}/\text{H}] < -1$  and  $[\text{O}, \text{Na}, \text{Mg}, \text{Al}, \text{K}, \text{Co}/\text{Fe}] < 0$ . Those elemental abundance ratios form the intersection of the IRMP criteria defined in Reggiani et al. (2023) and the list of elemental abundances reliably inferred for giant stars as part of APOGEE DR17.<sup>10</sup> For the purposes of the occurrence calculation described in the next section, an IRMP star with  $[\text{Fe}/\text{H}] < -1$  must have at least one non-null abundance ratio  $[\text{O}/\text{Fe}]$ ,  $[\text{Na}/\text{Fe}]$ ,  $[\text{Mg}/\text{Fe}]$ ,  $[\text{Al}/\text{Fe}]$ ,  $[\text{K}/\text{Fe}]$ , or  $[\text{Co}/\text{Fe}]$  and all abundance ratios  $[\text{O}, \text{Na}, \text{Mg}, \text{Al}, \text{K}, \text{Co}/\text{Fe}]$  either subsolar or null.

To accurately label stars with their correct galactic environments, we first join the APOGEE data described above with data from Gaia DR2 (Gaia Collaboration et al. 2016; Arenou et al. 2018; Evans et al. 2018; Gaia Collaboration et al. 2018; Lindegren et al. 2018; Luri et al. 2018; Riello et al. 2018) and DR3 (Gaia Collaboration et al. 2016; Lindegren et al. 2021a, 2021b; Fabricius et al. 2021; Gaia Collaboration et al. 2021; Riello et al. 2021; Rowell et al. 2021; Torra et al. 2021). We use the `apogee_id` string to identify the corresponding Gaia DR2 and DR3 `source_id` long integers by joining with the `gaiadr2.tmass_best_neighbour` and `gaiadr3.tmass_psc_xsc_best_neighbour` tables available in the Gaia archive (Salgado et al. 2017; Marrese et al. 2019). Occasionally multiple Gaia DR2 and DR3 `source_id` long integers are matched to the same object in the Two Micron All Sky Survey (2MASS) Point Source Catalog (Skrutskie et al. 2006). In those cases, we associate a 2MASS object with the closest Gaia DR2 and DR3 object that has (1) an absolute 2MASS  $K_s$ -band magnitude  $M_K < 2.31$  assuming Gaia DR2- or DR3-prior informed geometric distances (Bailer-Jones et al. 2018, 2021) and (2) Gaia-2MASS colors  $0.5 < G - J < 2.3$ ,  $0.6 < G - H < 3.3$ , and  $0.6 < G - K_s < 3.4$  predicted by the MESA Isochrones & Stellar Tracks (MIST) grid for metal-poor giants in the range  $-2.5 < [\text{Fe}/\text{H}] < -1.0$  (Paxton et al. 2011, 2013, 2015; Choi et al. 2016; Dotter 2016; Paxton et al. 2018).

We then use the Gaia DR2 `source_id` to identify Milky Way satellite classical dSph galaxies or Magellanic Cloud members using the Gaia DR2-based membership lists published in Gaia Collaboration et al. (2018). We identify globular cluster members using the Gaia DR3 `source_id` and the Vasiliev & Baumgardt (2021) lists of stars with globular cluster membership probability greater than 0.5, and this procedure results in a sample with at least one star from 41 globular clusters over the metallicity range  $-2.3 \lesssim [\text{Fe}/\text{H}] \lesssim -1.0$ .

Most stars observed as part of SDSS-III/APOGEE and SDSS-IV/APOGEE-2 were selected for observation by a procedure that sought to minimize age and metallicity biases (e.g., Zasowski et al. 2013, 2017), and we use the targeting flag `extratarg = 0` in the table `apogeeStar` to select those stars for our Milky Way field sample. To ensure the cleanest Milky Way field sample possible, we then remove from this sample any stars that are identified as dSph, Magellanic Cloud, or globular cluster members in Gaia Collaboration et al. (2018)

or Vasiliev & Baumgardt (2021). Because the vast majority of stars with  $[\text{Fe}/\text{H}] \lesssim -1$  observed as part of SDSS-III/APOGEE and SDSS-IV/APOGEE-2 are on halo-like orbits (e.g., Hayes et al. 2018), our Milky Way field sample can be thought of as a Milky Way halo sample. We list in Table 1 our entire analysis sample including IRMP status and galactic environment. We report in Table 2 the number of stars classified as IRMP stars in each environment,  $N_{*,\text{IRMP}}$ , along with the number of stars in our analysis sample in each environment,  $N_{*,\text{tot}}$ .

The typical elemental abundance inference uncertainties in our analysis sample are (0.04, 0.23, 0.03, 0.04, 0.08, 0.16) dex for ( $[\text{O}/\text{Fe}]$ ,  $[\text{Na}/\text{Fe}]$ ,  $[\text{Mg}/\text{Fe}]$ ,  $[\text{Al}/\text{Fe}]$ ,  $[\text{K}/\text{Fe}]$ ,  $[\text{Co}/\text{Fe}]$ ). In any case, elemental abundance inference uncertainties are irrelevant for the occurrence analyses presented in Section 3 if (1) the uncertainty distributions for each elemental abundance inference for each individual star are symmetric and (2) the uncertainty distributions have statistically indistinguishable widths across all of the galactic environments we explored. The individual elemental abundance inference uncertainties presented in the SDSS DR17 version of the table `aspcapStar` are reported as symmetric. Additionally, we confirmed that the individual elemental abundance uncertainty distributions for oxygen, sodium, magnesium, aluminum, potassium, and cobalt have statistically indistinguishable widths across all of the galactic environments we explored. Both of the conditions listed above are therefore met in our analysis sample. Likewise, we argue that our procedure to handle data quality issues will not bias the occurrence analyses we present in Section 3. The reason is that `null` values impact less than about 0.2% of the magnesium abundance inferences in our sample. Because we require all non-null elemental inferences to meet our IRMP criteria, we are able to exclude essentially all non-IRMP stars from our IRMP sample using magnesium alone almost regardless of data quality issues.

The recent discovery of a very metal-poor star with elemental abundances best explained by the nucleosynthesis expected in a pair-instability supernova has focused attention on that explanation for stars with significantly subsolar  $[\text{Na}/\text{Fe}]$  and  $[\alpha/\text{Fe}]$  abundance ratios (Xing et al. 2023). While the stars in our analysis sample have subsolar  $[\text{Na}/\text{Fe}]$  and the  $\alpha$ -element abundance ratios  $[\text{O}/\text{Fe}]$  and  $[\text{Mg}/\text{Fe}]$ , none of the stars in our sample have the strong odd-even abundance ratios predicted to be produced by pair-instability supernovae (e.g., Heger & Woosley 2002). We are therefore confident that the IRMP stars we identify are related to thermonuclear supernovae.

### 3. Analysis

We model the number of IRMP stars  $N_{*,\text{IRMP}}$  in a sample of  $N_{*,\text{tot}}$  candidates using a binomial distribution. Following Schlafman (2014), we exploit the fact that a Beta( $\alpha$ ,  $\beta$ ) distribution is a conjugate prior to the binomial distribution and will result in a Beta distribution posterior for the occurrence of IRMP stars in a sample. Bayes's theorem guarantees

$$f(\theta|\mathbf{y}) = \frac{f(\mathbf{y}|\theta)f(\theta)}{\int f(\mathbf{y}|\theta)f(\theta)d\theta}, \quad (1)$$

where  $f(\theta|\mathbf{y})$  is the posterior distribution of the model parameter  $\theta$ ,  $f(\mathbf{y}|\theta)$  is the likelihood of the data  $\mathbf{y}$  given  $\theta$ , and  $f(\theta)$  is the prior for  $\theta$ . In this case, the likelihood is the binomial likelihood

<sup>10</sup> <https://www.sdss4.org/dr17/irspec/abundances>

**Table 1**  
Analysis Sample

APOGEE ID	Gaia DR3 <i>source_id</i>	Gaia DR2 <i>source_id</i>	IRMP	Environment
2M17165079–2422565	4111066558908989184	4111066558908989184	False	Milky Way
2M17150296–2423503	4114045307692005632	4114045307692005632	False	Milky Way
2M19154424–0604209	4211181280154376320	4211181280154376320	False	Milky Way
2M19033822+1745138	4514220364269464832	4514220364269464832	False	Milky Way
2M16574858–2156135	4126283868512500864	4126283868512500864	False	Milky Way
2M18501947+2948368	2041393317228382848	2041393317228382848	False	Milky Way
2M18132084+0112054	4275831399934633984	4275831399934633984	False	Milky Way
2M17571005–3020262	4056215664653907456	4056215664653907456	False	Milky Way
2M17415271–2715374	4060889448072712832	4060889448072712832	False	Milky Way
2M19084424–0618527	4205916204326948736	4205916204326948736	False	Milky Way

(This table is available in its entirety in machine-readable form.)

**Table 2**  
Occurrence of IRMP Stars as a Function of Environment

Galactic Environment	$N_{*,\text{IRMP}}$	$N_{*,\text{tot}}$	Occurrence
Milky Way	5	4247	$0.0013^{+0.0006}_{-0.0005}$
<i>Globular clusters sum</i>	0	1998	$<0.00057$
LMC	4	203	$0.023^{+0.012}_{-0.009}$
SMC	24	572	$0.043^{+0.009}_{-0.008}$
<i>Magellanic Clouds sum</i>	28	775	$0.037^{+0.007}_{-0.006}$
Sagittarius	0	27	$<0.04$
Ursa Minor	0	8	$<0.12$
Sextans	1	6	$0.2^{+0.2}_{-0.1}$
Sculptor	8	70	$0.12^{+0.04}_{-0.03}$
Draco	0	9	$<0.11$
Carina	1	31	$0.05^{+0.05}_{-0.03}$
<i>dSph galaxies sum</i>	10	151	$0.07^{+0.02}_{-0.02}$

that describes the probability of a number of successes  $y$  in  $n$  Bernoulli trials each with probability  $\theta$  of success

$$f(y|\theta) = \binom{n}{y} \theta^y (1 - \theta)^{n-y}. \quad (2)$$

As shown by Schlafman (2014), in this situation using a Beta ( $\alpha$ ,  $\beta$ ) prior on  $\theta$  with hyperparameters  $\alpha$  and  $\beta$  results in a Beta posterior for  $\theta$  of the form  $\text{Beta}(\alpha + N_{*,\text{IRMP}}, \beta + N_{*,\text{tot}} - N_{*,\text{IRMP}})$ .

The hyperparameters  $\alpha$  and  $\beta$  of the prior can be thought of as encoding a certain amount of prior information in the form of pseudo-observations. Specifically,  $\alpha - 1$  is the number of successes and  $\beta - 1$  is the number of failures imagined to have already been observed and therefore included as prior information on  $\theta$ . Taking any  $\alpha = \beta = i$  where  $i \geq 1$  could be thought of as an uninformative prior in the sense that the probabilities of success and failure in the prior distribution are equally likely. However, if  $i$  is large, then there is imagined to be a lot of prior information and the posterior distribution will mostly reflect the prior when  $n \leq i$ . On the other hand, if  $n \gg i$ , then the posterior will be dominated by the data. For that reason, we take  $\alpha = \beta = 1$ .

We provide the posterior median occurrence of IRMP stars in each galactic environment in Table 2. We define the lower uncertainty as the difference between the posterior median and its 16th percentile. Likewise, we define the upper uncertainty as the

**Table 3**  
Occurrence Posterior Overlap Probabilities

Population	Population	$P(\text{Posterior Overlap})$
dSph galaxies	Magellanic Clouds	$1.095 \times 10^{-2}$
dSph galaxies	Milky Way field	$3.596 \times 10^{-16}$
Magellanic Clouds	Milky Way field	$1.620 \times 10^{-20}$
Milky Way field	Milky Way globular clusters	$4.300 \times 10^{-2}$

difference between the posterior’s 84th percentile and its median. For an environment with no IRMP stars, we report  $1\sigma$  upper limits as the 68th percentile of the posterior distribution. We find that  $\eta_{\text{dSph}} = 0.07^{+0.02}_{-0.02}$ ,  $\eta_{\text{Mag}} = 0.037^{+0.007}_{-0.006}$ ,  $\eta_{\text{MWF}} = 0.0013^{+0.0006}_{-0.0005}$ , and a  $1\sigma$  upper limit  $\eta_{\text{MWGC}} < 0.00057$ . In words, IRMP stars are much more common in the Milky Way’s classical dSph satellites and the Magellanic Clouds than in the Milky Way field or globular cluster populations. IRMP stars are less common in globular clusters than in any other galactic environment. We find that the overlap probability between the IRMP occurrences we observed in the Milky Way’s classical dSph satellites and the Magellanic Clouds is about 1 in 91, equivalent to about  $2.3\sigma$ . We find that the overlap probabilities between the IRMP occurrences we observe in the Milky Way’s classical dSph satellites and the Magellanic Clouds and the occurrence of IRMP stars we observe in the Milky Way field population are about 1 in  $2.8 \times 10^{15}$  and 1 in  $6.2 \times 10^{19}$ , equivalent to about  $8.1\sigma$  and  $9.2\sigma$ . The overlap probability between the IRMP occurrences we observe in the Milky Way field and globular cluster populations is about 1 in 23, equivalent to about  $1.7\sigma$ . We summarize these occurrence posterior overlap probabilities in Table 3.

The results presented in Table 2 are averaged over metallicity. To investigate IRMP occurrence as a function of metallicity, for each class of galactic environment we divide into 10 equal intervals the metallicity range spanned by our analysis sample for that environment. We then apply the same occurrence formalism in each individual metallicity interval and plot occurrence as a function of metallicity for each environment in Figure 1. We find no significant dependence of the occurrence of IRMP stars on metallicity in our analysis sample.

#### 4. Discussion

We find that the occurrences of IRMP stars in the Milky Way’s satellite classical dSph galaxies, the Magellanic Clouds,

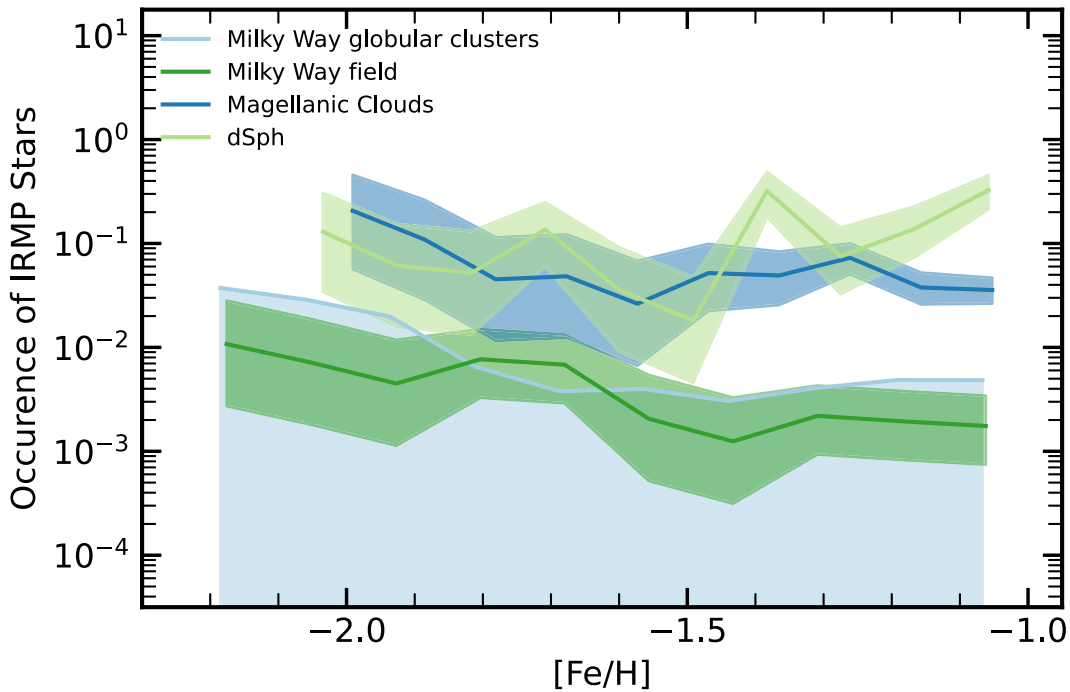


**Figure 1.** Occurrence of IRMP stars as a function of metallicity in different environments. For the Milky Way field, dSph, and Magellanic Cloud samples we plot the posterior medians of occurrence as solid lines and the ranges defined by the 16th and 84th percentiles of the occurrence posteriors as transparent polygons. For the globular cluster sample for which we infer an upper limit on iron-rich metal-poor (IRMP) occurrence, we plot the 68th percentile of the posterior as a solid line and the range defined by the 0th and 68th percentiles of the occurrence posterior as a transparent polygon. There is no obvious dependence of IRMP occurrence on metallicity in the Milky Way’s field population, its globular clusters, its classical dSph galaxies, or the Magellanic Clouds.

the Milky Way field population, and the Milky Way’s globular cluster populations have the values  $\eta_{\text{dSph}} = 0.07^{+0.02}_{-0.02}$ ,  $\eta_{\text{Mag}} = 0.037^{+0.007}_{-0.006}$ ,  $\eta_{\text{MWF}} = 0.0013^{+0.0006}_{-0.0005}$ , and  $\eta_{\text{MWGC}} < 0.00057$ , respectively. The probability that the IRMP occurrences in the Milky Way’s satellite classical dSph galaxies and the Magellanic Clouds overlap is about 1 in 91, equivalent to about  $2.3\sigma$ . The probabilities that the IRMP occurrence posterior for the Milky Way field overlaps with the IRMP occurrence posteriors for Milky Way’s satellite classical dSph galaxies and the Magellanic Clouds are about 1 in  $2.8 \times 10^{15}$  and 1 in  $6.2 \times 10^{19}$ , respectively, equivalent to about  $8.1\sigma$  and  $9.2\sigma$ . The probability that the IRMP occurrences in the Milky Way field and globular cluster populations overlap is about 1 in 23, equivalent to about  $1.7\sigma$ . While the absolute values of IRMP star occurrences may be difficult to interpret, as we argued in the introduction, their ordering  $\eta_{\text{MWGC}} \sim \eta_{\text{MWF}} < \eta_{\text{Mag}} \sim \eta_{\text{dSph}}$  has two important implications.

The increased occurrence of IRMP stars in environments like the Milky Way’s satellite classical dSph galaxies and the Magellanic Clouds, where thermonuclear supernovae were important contributors to chemical evolution, supports the Reggiani et al. (2023) scenario for IRMP star formation in molecular cores with metal contents dominated by the thermonuclear supernova nucleosynthesis. The confirmation of this Reggiani et al. (2023) prediction reinforces the idea that the elemental abundances of individual IRMP stars can be used to investigate the progenitor systems and explosion mechanisms responsible for the thermonuclear supernovae that produced much of their metal contents.

The statistically indistinguishable occurrences of IRMP stars in the Milky Way’s field and globular cluster populations

suggest that the time lags between the formation of globular clusters’ first and second stellar generations were longer than the thermonuclear supernova delay time. This is broadly consistent with the idea from the asymptotic giant branch (AGB) scenario for globular cluster multiple populations that the explosions of thermonuclear supernovae associated with a globular cluster’s first stellar generation quench the star formation event that produced its second stellar generation (e.g., D’Ercole et al. 2008; Calura et al. 2019; Lacchin et al. 2021). Given the suspected importance of thermonuclear supernovae for quenching second-generation star formation in globular clusters, it remains to be explained why globular cluster second-generation stars that bear the imprint of thermonuclear supernova nucleosynthesis are so rare as to not appear in a sample of nearly 2000 globular cluster members. Our result is also consistent with scenarios for globular cluster multiple populations invoking a thermonuclear supernova at the start of a cluster’s evolution (e.g., Marcolini et al. 2009; Sánchez-Blázquez et al. 2012).

Contributions from both core-collapse and thermonuclear supernovae, as well as *s*- and *r*-process nucleosynthesis, are required to explain the solar abundance pattern. While the progenitors of core-collapse supernovae are known to be massive stars and the *s*-process takes place in AGB stars, the progenitors of thermonuclear supernovae and the astrophysical site of the *r*-process are more uncertain. Observational constraints on either the progenitors of thermonuclear supernovae or the astrophysical site of the *r*-process are therefore valuable. The kilonova GW170817 confirmed that neutron star mergers are at least partially responsible for *r*-process nucleosynthesis (e.g., Abbott et al. 2017; Arcavi et al. 2017). The relative occurrences of IRMP and *r*-process-enhanced stars

in the same populations can be used to compare the relative probabilities of the circumstances that lead to the formation of IRMP and  $r$ -process-enhanced stars.

We find that the occurrences of IRMP stars are an order of magnitude lower than the occurrence of  $r$ -process-enhanced stars in both the Milky Way field and Magellanic Clouds. In the Milky Way field, we find that  $\eta_{\text{IRMP,MWF}} = 0.0013^{+0.0006}_{-0.0005}$ , while Barklem et al. (2005) found  $\eta_{\text{rII,MWF}} \approx 0.03$  according to the definition of highly  $r$ -process-enhanced stars (i.e.,  $r$ -II stars) from Beers & Christlieb (2005).<sup>11</sup> In the Magellanic Clouds, we find that  $\eta_{\text{IRMP,Mag}} = 0.037^{+0.007}_{-0.006}$ , while Reggiani et al. (2021) found  $\eta_{\text{rII,Mag}} = 0.38^{+0.14}_{-0.13}$ . We conclude that the circumstances that lead to the formation of IRMP stars occur an order of magnitude less frequently than the circumstances that lead to the formation of  $r$ -process-enhanced stars.

## 5. Conclusion

We conclude that iron-rich metal-poor (IRMP) stars with  $[\text{Fe}/\text{H}] \lesssim -1$  and  $[\text{O}, \text{Na}, \text{Mg}, \text{Al}, \text{K}, \text{Co}/\text{Fe}] < 0$  are more common in the Milky Way’s satellite classical dSph galaxies and the Magellanic Clouds than in the Milky Way field or globular cluster populations. Because thermonuclear supernovae are thought to have been more important contributors to the chemical evolution of the Milky Way’s satellite classical dSph galaxies and the Magellanic Clouds than to the Milky Way field and globular cluster populations in the range  $[\text{Fe}/\text{H}] \lesssim -1$ , our inferences confirm the interpretation of IRMP stars put forward in Reggiani et al. (2023) proposing that IRMP stars formed from molecular cores with metal contents dominated by thermonuclear supernova nucleosynthesis. IRMP stars can therefore be used to constrain the progenitor systems and explosion mechanisms of the thermonuclear supernovae responsible for their elemental abundances. We further find that the occurrences of IRMP stars in the Milky Way’s field and globular cluster populations are statistically indistinguishable. This observation implies that the time lag between the formation of a globular cluster’s first and second stellar generations was longer than the thermonuclear supernova delay time. It is also consistent with explanations for globular cluster multiple populations that require early enrichment by thermonuclear supernovae.

## Acknowledgments

We thank Yossef Zenati for sharing his expertise on Type Ia supernovae. Support for this work was provided by Johns Hopkins University through a Summer Provost’s Undergraduate Research Award to Zachary Reeves and by the Carnegie Institution for Science through a Carnegie Postdoctoral Fellowship award to Henrique Reggiani. Funding for SDSS-III has been provided by the Alfred P. Sloan Foundation, the Participating Institutions, the National Science Foundation, and the U.S. Department of Energy Office of Science. The SDSS-III website is <http://www.sdss3.org/>. SDSS-III is managed by the Astrophysical Research Consortium for the Participating Institutions of the SDSS-III Collaboration, including the University of Arizona, the Brazilian Participation Group, Brookhaven National Laboratory, Carnegie Mellon University, University of Florida, the French Participation Group, the German Participation Group, Harvard

University, the Instituto de Astrofísica de Canarias, the Michigan State/Notre Dame/JINA Participation Group, Johns Hopkins University, Lawrence Berkeley National Laboratory, Max Planck Institute for Astrophysics, Max Planck Institute for Extraterrestrial Physics, New Mexico State University, New York University, The Ohio State University, Pennsylvania State University, University of Portsmouth, Princeton University, the Spanish Participation Group, University of Tokyo, University of Utah, Vanderbilt University, University of Virginia, University of Washington, and Yale University. Funding for the Sloan Digital Sky Survey IV has been provided by the Alfred P. Sloan Foundation, the U.S. Department of Energy Office of Science, and the Participating Institutions. SDSS-IV acknowledges support and resources from the Center for High Performance Computing at the University of Utah. The SDSS website is [www.sdss.org](http://www.sdss.org). SDSS-IV is managed by the Astrophysical Research Consortium for the Participating Institutions of the SDSS Collaboration, including the Brazilian Participation Group, the Carnegie Institution for Science, Carnegie Mellon University, Center for Astrophysics—Harvard & Smithsonian, the Chilean Participation Group, the French Participation Group, Instituto de Astrofísica de Canarias, Johns Hopkins University, Kavli Institute for the Physics and Mathematics of the Universe (IPMU)/University of Tokyo, the Korean Participation Group, Lawrence Berkeley National Laboratory, Leibniz Institut für Astrophysik Potsdam (AIP), Max-Planck-Institut für Astronomie (MPIA Heidelberg), Max-Planck-Institut für Astrophysik (MPA Garching), Max-Planck-Institut für Extraterrestrische Physik (MPE), National Astronomical Observatories of China, New Mexico State University, New York University, University of Notre Dame, Observatório Nacional/MCTI, The Ohio State University, Pennsylvania State University, Shanghai Astronomical Observatory, United Kingdom Participation Group, Universidad Nacional Autónoma de México, University of Arizona, University of Colorado Boulder, University of Oxford, University of Portsmouth, University of Utah, University of Virginia, University of Washington, University of Wisconsin, Vanderbilt University, and Yale University. This work has made use of data from the European Space Agency (ESA) mission Gaia (<https://www.cosmos.esa.int/gaia>), processed by the Gaia Data Processing and Analysis Consortium (DPAC, <https://www.cosmos.esa.int/web/gaia/dpac/consortium>). Funding for the DPAC has been provided by national institutions, in particular the institutions participating in the Gaia Multilateral Agreement. This publication makes use of data products from the Two Micron All Sky Survey, which is a joint project of the University of Massachusetts and the Infrared Processing and Analysis Center/California Institute of Technology, funded by the National Aeronautics and Space Administration and the National Science Foundation. This research has made use of the SIMBAD database, operated at CDS, Strasbourg, France (Wenger et al. 2000). This research has made use of the VizieR catalog access tool, CDS, Strasbourg, France. The original description of the VizieR service was published in Ochsenbein et al. (2000). This research has made use of NASA’s Astrophysics Data System Bibliographic Services.

*Facilities:* CDS, CTIO:2MASS, Du Pont (APOGEE), FLWO:2MASS, Gaia, Sloan (APOGEE).

*Software:* *astropy* (Astropy Collaboration et al. 2013, 2018), *matplotlib* (Hunter 2007) *numpy* (Harris et al. 2020), *pandas* (McKinney et al. 2019; pandas Development Team 2020), *R* (R Core Team 2023), *scipy* (Virtanen et al. 2020).

<sup>11</sup> More recent estimates by the  $R$ -Process Alliance have found similar occurrences (e.g., Hansen et al. 2018; Sakari et al. 2018; Ezzeddine et al. 2020).

## Appendix

SDSS DR17 APOGEE data quality and targeting information are stored as bitmasks.<sup>12</sup> Since unreliable photospheric stellar parameters will lead to unreliable elemental abundances, we exclude from our analysis stars with the bits `TEFF_WARN`, `LOGG_WARN`, `VMICRO_WARN`, `M_H_WARN`, `STAR_WARN`, `CHI2_WARN`, `COLORTE_WARN`, `ROTATION_WARN`, `SN_WARN`, `TEFF_BAD`, `LOGG_BAD`, `VMICRO_BAD`, `M_H_BAD`, `STAR_BAD`, `CHI2_BAD`, `COLORTE_BAD`, `ROTATION_BAD`, or `SN_BAD` set in the column `aspcapflag` in the table `aspcapStar`. These flags correspond to binary digits 0, 1, 2, 3, 7, 8, 9, 10, 11, 16, 17, 18, 19, 23, 24, 25, 26, and 27. Note that though the bit corresponding to `STAR_WARN` should be set if any of the bits `TEFF_WARN`, `LOGG_WARN`, `CHI2_WARN`, `COLORTE_WARN`, `ROTATION_WARN`, or `SN_WARN` are set, we choose to include all of these bits in our data quality checks. Likewise, though the bit corresponding to `STAR_BAD` should be set if any of the bits `TEFF_BAD`, `LOGG_BAD`, `CHI2_BAD`, `COLORTE_BAD`, `ROTATION_BAD`, or `SN_BAD` are set, we choose to include all of these bits in our data quality checks. We remove duplicate observations from our analysis sample by rejecting objects with binary digit 4 set in the column `extratarg` in the table `apogeeStar`.

We exclude from our analysis any elemental abundances that are indicated as suspect. We set to null all elemental abundances with the final value `-9999` or with any of the bits `GRIDEDGE_BAD`, `CALRANGE_BAD`, `OTHER_BAD`, `FERRE_FAIL`, `PARAM_MISMATCH_BAD`, `TEFF_CUT`, `GRIDEDGE_WARN`, `CALRANGE_WARN`, `OTHER_WARN`, `PARAM_MISMATCH_WARN`, `ERR_WARN`, or `PARAM_FIXED` set in a column `*_fe_flag` in the table `aspcapStar`. These flags correspond to binary digits 0, 1, 2, 3, 4, 6, 8, 9, 10, 12, 14, and 16. We ultimately use the following query in the `CasJobs` portal to generate our analysis sample:

```
SELECT a.apogee_id, b.ra, b.dec, b.glon, b.
  glat, b.snr, b.extratarg,
CASE WHEN ((a.teff_flag & 87903)=0) AND (a.
  teff > -9999)
THEN a.teff ELSE null END AS teff,
CASE WHEN ((a.teff_flag & 87903)=0) AND (a.
  teff > -9999)
THEN a.teff_err ELSE null END AS teff_err,
CASE WHEN ((a.logg_flag & 87903)=0) AND (a.
  logg > -9999)
THEN a.logg ELSE null END AS logg,
CASE WHEN ((a.logg_flag & 87903)=0) AND (a.
  logg > -9999)
THEN a.logg_err ELSE null END AS logg_err,
CASE WHEN ((a.m_h_flag & 87903)=0) AND (a.
  m_h > -9999)
THEN a.m_h ELSE null END AS m_h,
CASE WHEN ((a.m_h_flag & 87903)=0) AND (a.
  m_h > -9999)
THEN a.m_h_err ELSE null END AS m_h_err,
CASE WHEN (((a.fe_h_flag & 87903)=0) AND
  (fe_h > -9999))
THEN fe_h ELSE null END AS fe_h,
CASE WHEN (((a.fe_h_flag & 87903)=0) AND
  (fe_h > -9999))
```

```
THEN fe_h_err ELSE null END AS fe_h_err,
CASE WHEN (((a.o_fe_flag & 87903)=0) AND
  ((a.fe_h_flag & 87903)=0)
AND (a.o_fe > -9999) AND (a.fe_h > -9999))
THEN a.o_fe ELSE null END AS o_fe,
CASE WHEN (((a.o_fe_flag & 87903)=0) AND
  ((a.fe_h_flag & 87903)=0)
AND (a.o_fe > -9999) AND (a.fe_h > -9999))
THEN a.o_fe_err ELSE null END AS o_fe_err,
CASE WHEN (((a.na_fe_flag & 87903)=0) AND
  ((a.fe_h_flag & 87903)=0)
AND (a.na_fe > -9999) AND (a.fe_h > -9999))
THEN a.na_fe ELSE null END AS na_fe,
CASE WHEN (((a.na_fe_flag & 87903)=0) AND
  ((a.fe_h_flag & 87903)=0)
AND (a.na_fe > -9999) AND (a.fe_h > -9999))
THEN a.na_fe_err ELSE null END AS na_fe_err,
CASE WHEN (((a.mg_fe_flag & 87903)=0) AND
  ((a.fe_h_flag & 87903)=0)
AND (a.mg_fe > -9999) AND (a.fe_h > -9999))
THEN a.mg_fe ELSE null END AS mg_fe,
CASE WHEN (((a.mg_fe_flag & 87903)=0) AND
  ((a.fe_h_flag & 87903)=0)
AND (a.mg_fe > -9999) AND (a.fe_h > -9999))
THEN a.mg_fe_err ELSE null END AS mg_fe_err,
CASE WHEN (((a.al_fe_flag & 87903)=0) AND
  ((a.fe_h_flag & 87903)=0)
AND (a.al_fe > -9999) AND (a.fe_h > -9999))
THEN a.al_fe ELSE null END AS al_fe,
CASE WHEN (((a.al_fe_flag & 87903)=0) AND
  ((a.fe_h_flag & 87903)=0)
AND (a.al_fe > -9999) AND (a.fe_h > -9999))
THEN a.al_fe_err ELSE null END AS al_fe_err,
CASE WHEN (((a.k_fe_flag & 87903)=0) AND
  ((a.fe_h_flag & 87903)=0)
AND (a.k_fe > -9999) AND (a.fe_h > -9999))
THEN a.k_fe ELSE null END AS k_fe,
CASE WHEN (((a.k_fe_flag & 87903)=0) AND
  ((a.fe_h_flag & 87903)=0)
AND (a.k_fe > -9999) AND (a.fe_h > -9999))
THEN a.k_fe_err ELSE null END AS k_fe_err,
CASE WHEN (((a.co_fe_flag & 87903)=0) AND
  ((a.fe_h_flag & 87903)=0)
AND (a.co_fe > -9999) AND (a.fe_h > -9999))
THEN a.co_fe ELSE null END AS co_fe,
CASE WHEN (((a.co_fe_flag & 87903)=0) AND
  ((a.fe_h_flag & 87903)=0)
AND (a.co_fe > -9999) AND (a.fe_h > -9999))
THEN a.co_fe_err ELSE null END AS co_fe_err
FROM DR17.aspcapStar a
INNER JOIN DR17.apogeeStar b ON a.apstar_
  id=b.apstar_id
WHERE (a.aspcapflag & 261033871)=0
AND (b.extratarg & 16)=0
AND a.logg < 3.8
```

## ORCID iDs

Zachary Reeves  <https://orcid.org/0000-0002-0821-878X>  
 Kevin C. Schlafman  <https://orcid.org/0000-0001-5761-6779>

<sup>12</sup> <https://www.sdss4.org/dr17/irspec/apogee-bitmasks>

Henrique Reggiani  <https://orcid.org/0000-0001-6533-6179>

## References

- Abbott, B. P., Abbott, R., Abbott, T. D., et al. 2017, *PhRvL*, **119**, 161101
- Abdurro'uf, Accetta, K., Aerts, C., et al. 2022, *ApJS*, **259**, 35
- Allende Prieto, C., Beers, T. C., Wilhelm, R., et al. 2006, *ApJ*, **636**, 804
- Alvarez, R., & Plez, B. 1998, *A&A*, **330**, 1109
- Arcavi, I., Hosseinzadeh, G., Howell, D. A., et al. 2017, *Natur*, **551**, 64
- Arenou, F., Luri, X., Babusiaux, C., et al. 2018, *A&A*, **616**, A17
- Astropy Collaboration, Price-Whelan, A. M., Sipőcz, B. M., et al. 2018, *AJ*, **156**, 123
- Astropy Collaboration, Robitaille, T. P., Tollerud, E. J., et al. 2013, *A&A*, **558**, A33
- Bailer-Jones, C. A. L., Rybizki, J., Fousneau, M., Demleitner, M., & Andrae, R. 2021, *AJ*, **161**, 147
- Bailer-Jones, C. A. L., Rybizki, J., Fousneau, M., Mantelet, G., & Andrae, R. 2018, *AJ*, **156**, 58
- Barklem, P. S., Christlieb, N., Beers, T. C., et al. 2005, *A&A*, **439**, 129
- Bastian, N., & Lardo, C. 2018, *ARA&A*, **56**, 83
- Beaton, R. L., Oelkers, R. J., Hayes, C. R., et al. 2021, *AJ*, **162**, 302
- Beers, T. C., & Christlieb, N. 2005, *ARA&A*, **43**, 531
- Bekki, K., & Tsujimoto, T. 2012, *ApJ*, **761**, 180
- Blanton, M. R., Bershad, M. A., Abolfathi, B., et al. 2017, *AJ*, **154**, 28
- Boos, S. J., Townsley, D. M., Shen, K. J., Caldwell, S., & Miles, B. J. 2021, *ApJ*, **919**, 126
- Bowen, I. S., & Vaughan, A. H. J. 1973, *ApOpt*, **12**, 1430
- Bravo, E., Badenes, C., & Martínez-Rodríguez, H. 2019, *MNRAS*, **482**, 4346
- Calura, F., D'Ercole, A., Vesperini, E., Vanzella, E., & Sollima, A. 2019, *MNRAS*, **489**, 3269
- Carney, B. W., Latham, D. W., Stefanik, R. P., Laird, J. B., & Morse, J. A. 2003, *AJ*, **125**, 293
- Carretta, E., Bragaglia, A., Gratton, R. G., et al. 2009, *A&A*, **505**, 117
- Choi, J., Dotter, A., Conroy, C., et al. 2016, *ApJ*, **823**, 102
- Cohen, J. G. 1978, *ApJ*, **223**, 487
- Cohen, J. G. 1979, *ApJ*, **231**, 751
- Cohen, J. G. 1980, *ApJ*, **241**, 981
- Cohen, J. G. 1981, *ApJ*, **247**, 869
- Conroy, C. 2012, *ApJ*, **758**, 21
- Cunha, K., Smith, V. V., Johnson, J. A., et al. 2015, *ApJL*, **798**, L41
- D'Ercole, A., Vesperini, E., D'Antona, F., McMillan, S. L. W., & Recchi, S. 2008, *MNRAS*, **391**, 825
- Dotter, A. 2016, *ApJS*, **222**, 8
- Eisenstein, D. J., Weinberg, D. H., Agol, E., et al. 2011, *AJ*, **142**, 72
- Evans, D. W., Riello, M., De Angeli, F., et al. 2018, *A&A*, **616**, A4
- Ezzeddine, R., Rasmussen, K., Frebel, A., et al. 2020, *ApJ*, **898**, 150
- Fabrizius, C., Luri, X., Arenou, F., et al. 2021, *A&A*, **649**, A5
- Fink, M., Kromer, M., Seitzzahl, I. R., et al. 2014, *MNRAS*, **438**, 1762
- Gaia Collaboration, Brown, A. G. A., Vallenari, A., et al. 2021, *A&A*, **649**, A1
- Gaia Collaboration, Helmi, A., van Leeuwen, F., et al. 2018, *A&A*, **616**, A12
- Gaia Collaboration, Prusti, T., de Bruijne, J. H. J., et al. 2016, *A&A*, **595**, A1
- García Pérez, A. E., Allende Prieto, C., Holtzman, J. A., et al. 2016, *AJ*, **151**, 144
- Gratton, R., Sneden, C., & Carretta, E. 2004, *ARA&A*, **42**, 385
- Gratton, R. G. 1983, *A&A*, **123**, 289
- Gratton, R. G., Bonifacio, P., Bragaglia, A., et al. 2001, *A&A*, **369**, 87
- Gratton, R. G., & Ortolani, S. 1986, *A&A*, **169**, 201
- Gratton, R. G., & Sneden, C. 1988, *A&A*, **204**, 193
- Graur, O., Rodney, S. A., Maoz, D., et al. 2014, *ApJ*, **783**, 28
- Gronow, S., Collins, C. E., Sim, S. A., & Röpke, F. K. 2021a, *A&A*, **649**, A155
- Gronow, S., Côté, B., Lach, F., et al. 2021b, *A&A*, **656**, A94
- Gunn, J. E., Siegmund, W. A., Mannery, E. J., et al. 2006, *AJ*, **131**, 2332
- Gustafsson, B., Edvardsson, B., Eriksson, K., et al. 2008, *A&A*, **486**, 951
- Hansen, T. T., Holmbeck, E. M., Beers, T. C., et al. 2018, *ApJ*, **858**, 92
- Harris, C. R., Millman, K. J., van der Walt, S. J., et al. 2020, *Natur*, **585**, 357
- Hayes, C. R., Majewski, S. R., Shetrone, M., et al. 2018, *ApJ*, **852**, 49
- Heger, A., & Woosley, S. E. 2002, *ApJ*, **567**, 532
- Holtzman, J. A., Harrison, T. E., & Coughlin, J. L. 2010, *AdAst*, **2010**, 193086
- Holtzman, J. A., Shetrone, M., Johnson, J. A., et al. 2015, *AJ*, **150**, 148
- Hubeny, I., & Lanz, T. 2011, Synspec: General Spectrum Synthesis Program, Astrophysics Source Code Library, ascl:1109.022
- Hunter, J. D. 2007, *CSE*, **9**, 90
- Jönsson, H., Holtzman, J. A., Allende Prieto, C., et al. 2020, *AJ*, **160**, 120
- Kirby, E. N., Cohen, J. G., Smith, G. H., et al. 2011a, *ApJ*, **727**, 79
- Kirby, E. N., Guhathakurta, P., Bolte, M., Sneden, C., & Geha, M. C. 2009, *ApJ*, **705**, 328
- Kirby, E. N., Guhathakurta, P., Simon, J. D., et al. 2010, *ApJS*, **191**, 352
- Kirby, E. N., Lanfranchi, G. A., Simon, J. D., Cohen, J. G., & Guhathakurta, P. 2011b, *ApJ*, **727**, 78
- Lacchin, E., Calura, F., & Vesperini, E. 2021, *MNRAS*, **506**, 5951
- Lanfranchi, G. A., & Matteucci, F. 2003, *MNRAS*, **345**, 71
- Lanfranchi, G. A., & Matteucci, F. 2004, *MNRAS*, **351**, 1338
- Lanfranchi, G. A., & Matteucci, F. 2007, *A&A*, **468**, 927
- Lanfranchi, G. A., Matteucci, F., & Cescutti, G. 2006, *A&A*, **453**, 67
- Lanfranchi, G. A., Matteucci, F., & Cescutti, G. 2008, *A&A*, **481**, 635
- Leung, S.-C., & Nomoto, K. 2018, *ApJ*, **861**, 143
- Leung, S.-C., & Nomoto, K. 2020a, *ApJ*, **888**, 80
- Leung, S.-C., & Nomoto, K. 2020b, *ApJ*, **900**, 54
- Lindgren, L., Bastian, U., Biermann, M., et al. 2021a, *A&A*, **649**, A4
- Lindgren, L., Hernández, J., Bombrun, A., et al. 2018, *A&A*, **616**, A2
- Lindgren, L., Klioner, S. A., Hernández, J., et al. 2021b, *A&A*, **649**, A2
- Lucatello, S., Sollima, A., Gratton, R., et al. 2015, *A&A*, **584**, A52
- Luck, R. E., & Bond, H. E. 1981, *ApJ*, **244**, 919
- Luck, R. E., & Bond, H. E. 1985, *ApJ*, **292**, 559
- Luri, X., Brown, A. G. A., Sarro, L. M., et al. 2018, *A&A*, **616**, A9
- Magain, P. 1985, *A&A*, **146**, 95
- Magain, P. 1989, *A&A*, **209**, 211
- Majewski, S. R., Schiavon, R. P., Frinchaboy, P. M., et al. 2017, *AJ*, **154**, 94
- Maoz, D., Mannucci, F., & Brandt, T. D. 2012, *MNRAS*, **426**, 3282
- Maoz, D., Mannucci, F., Li, W., et al. 2011, *MNRAS*, **412**, 1508
- Maoz, D., Mannucci, F., & Nelemans, G. 2014, *ARA&A*, **52**, 107
- Marcolini, A., D'Ercole, A., Brighenti, F., & Recchi, S. 2006, *MNRAS*, **371**, 643
- Marcolini, A., Gibson, B. K., Karakas, A. I., & Sánchez-Blázquez, P. 2009, *MNRAS*, **395**, 719
- Marrese, P. M., Marinoni, S., Fabrizio, M., & Altavilla, G. 2019, *A&A*, **621**, A144
- McKinney, W. 2019, in Proc. 9th Python in Science Conf., 621, ed. S. van der Walt & J. Millman (Austin, TX: SciPy), 56
- McWilliam, A., Preston, G. W., Sneden, C., & Searle, L. 1995a, *AJ*, **109**, 2757
- McWilliam, A., Preston, G. W., Sneden, C., & Shectman, S. 1995b, *AJ*, **109**, 2736
- Neopane, S., Bhargava, K., Fisher, R., et al. 2022, *ApJ*, **925**, 92
- Nidever, D. L., Hasselquist, S., Hayes, C. R., et al. 2020, *ApJ*, **895**, 88
- Nidever, D. L., Holtzman, J. A., Allende Prieto, C., et al. 2015, *AJ*, **150**, 173
- Nomoto, K., & Leung, S.-C. 2018, *SSRv*, **214**, 67
- Ochsenbeim, F., Bauer, P., & Marcout, J. 2000, *A&AS*, **143**, 23
- Ohlmann, S. T., Kromer, M., Fink, M., et al. 2014, *A&A*, **572**, A57
- Osorio, Y., Allende Prieto, C., Hubeny, I., Mészáros, S., & Shetrone, M. 2020, *A&A*, **637**, A80
- pandas Development Team 2020, pandas-dev/pandas: Pandas, v1.5.3, Zenodo, doi:10.5281/zenodo.3509134
- Papish, O., & Perets, H. B. 2016, *ApJ*, **822**, 19
- Paxton, B., Bildsten, L., Dotter, A., et al. 2011, *ApJS*, **192**, 3
- Paxton, B., Cantiello, M., Arras, P., et al. 2013, *ApJS*, **208**, 4
- Paxton, B., Marchant, P., Schwab, J., et al. 2015, *ApJS*, **220**, 15
- Paxton, B., Schwab, J., Bauer, E. B., et al. 2018, *ApJS*, **234**, 34
- Peterson, R. C. 1981, *ApJ*, **244**, 989
- Pilachowski, C. A., Sneden, C., & Wallerstein, G. 1983, *ApJS*, **52**, 241
- Plez, B. 2012, Turbospectrum: Code for spectral synthesis, Astrophysics Source Code Library, ascl:1205.004
- Pompéia, L., Hill, V., Spite, M., et al. 2008, *A&A*, **480**, 379
- R Core Team 2023, R: A Language and Environment for Statistical Computing, R Foundation for Statistical Computing, Vienna, Austria, <https://www.R-project.org/>
- Reggiani, H., Schlafman, K. C., & Casey, A. R. 2023, arXiv:2303.16357
- Reggiani, H., Schlafman, K. C., Casey, A. R., Simon, J. D., & Ji, A. P. 2021, *AJ*, **162**, 229
- Riello, M., De Angeli, F., Evans, D. W., et al. 2018, *A&A*, **616**, A3
- Riello, M., De Angeli, F., Evans, D. W., et al. 2021, *A&A*, **649**, A3
- Rowell, N., Davidson, M., Lindgren, L., et al. 2021, *A&A*, **649**, A11
- Ryan, S. G., Norris, J. E., & Bessell, M. S. 1991, *AJ*, **102**, 303
- Sakari, C. M., Placco, V. M., Farrell, E. M., et al. 2018, *ApJ*, **868**, 110
- Salgado, J., González-Núñez, J., Gutiérrez-Sánchez, R., et al. 2017, *A&C*, **21**, 22
- Sánchez-Blázquez, P., Marcolini, A., Gibson, B. K., et al. 2012, *MNRAS*, **419**, 1376
- Santana, F. A., Beaton, R. L., Covey, K. R., et al. 2021, *AJ*, **162**, 303

- Schlaufman, K. C. 2014, [ApJ](#), **790**, 91
- Seitzzahl, I. R., Ciaraldi-Schoolmann, F., Röpke, F. K., et al. 2013, [MNRAS](#), **429**, 1156
- Seitzzahl, I. R., Kromer, M., Ohlmann, S. T., et al. 2016, [A&A](#), **592**, A57
- Shetrone, M., Bizyaev, D., Lawler, J. E., et al. 2015, [ApJS](#), **221**, 24
- Shetrone, M., Venn, K. A., Tolstoy, E., et al. 2003, [AJ](#), **125**, 684
- Shetrone, M. D., Côté, P., & Sargent, W. L. W. 2001, [ApJ](#), **548**, 592
- Skrutskie, M. F., Cutri, R. M., Stiening, R., et al. 2006, [AJ](#), **131**, 1163
- Smith, V. V., Bizyaev, D., Cunha, K., et al. 2021, [AJ](#), **161**, 254
- Smith, V. V., Cunha, K., Shetrone, M. D., et al. 2013, [ApJ](#), **765**, 16
- Snedden, C., Kraft, R. P., Prosser, C. F., & Langer, G. E. 1992, [AJ](#), **104**, 2121
- Sukhbold, T., Ertl, T., Woosley, S. E., Brown, J. M., & Janka, H. T. 2016, [ApJ](#), **821**, 38
- Tolstoy, E., Venn, K. A., Shetrone, M., et al. 2003, [AJ](#), **125**, 707
- Torra, F., Castañeda, J., Fabricius, C., et al. 2021, [A&A](#), **649**, A10
- Totani, T., Morokuma, T., Oda, T., Doi, M., & Yasuda, N. 2008, [PASJ](#), **60**, 1327
- Van der Swaelmen, M., Hill, V., Primas, F., & Cole, A. A. 2013, [A&A](#), **560**, A44
- Vasiliev, E., & Baumgardt, H. 2021, [MNRAS](#), **505**, 5978
- Virtanen, P., Gommers, R., Oliphant, T. E., et al. 2020, [Nature Methods](#), **17**, 261
- Wallerstein, G. 1962, [ApJS](#), **6**, 407
- Wenger, M., Ochsenbein, F., Egret, D., et al. 2000, [A&AS](#), **143**, 9
- Wilson, J. C., Hearty, F. R., Skrutskie, M. F., et al. 2019, [PASP](#), **131**, 055001
- Xing, Q.-F., Zhao, G., Liu, Z.-W., et al. 2023, [Natur](#), **618**, 712
- Zasowski, G., Cohen, R. E., Chojnowski, S. D., et al. 2017, [AJ](#), **154**, 198
- Zasowski, G., Johnson, J. A., Frinchaboy, P. M., et al. 2013, [AJ](#), **146**, 81